SEGMENTED ELECTRODIFFUSION PROBES: SIMULTANEOUS MEASUREMENT OF SHEAR RATE AND NORMAL FLOW COMPONENT

Ondřej WEIN and Václav SOBOLÍK

Institute of Chemical Process Fundamentals,
Czechoslovak Academy of Sciences, 165 02 Prague 6-Suchdol

Received January 11, 1989
Accepted March 16, 1989

Dedicated to late Academician Eduard Hála.

The existing theory of direction-sensitive electrodiffusion probes for the wall shear rate measurement is extended by including normal flow effects.

Circular electrodiffusion probes consisting of three segments have been used recently for the measurements of wall shear rates in two-phase gas–liquid flows[1,2]. The response of such probes consists of three current signals. By treating simultaneously this multiple signal, it is possible to determine both the magnitude and direction of vectorial wall shear rate[3]. Until now, the treatment of the multiple current signal has been based on the calibration data obtained under viscometric conditions[4], i.e. in a steady unidirectional flow with constant wall shear rate.

Such conditions can be met neither in two-phase nor turbulent flows. Particles, bubbles, or turbulent eddies generate three-dimensional fluctuating flow structures even in the close proximity of walls. A question arises of interpreting the multiple current signal produced by the segmented probes under such nontrivial circumstances. From the deterministic point of view, the complicating factors can be understood as a superposition of velocity fluctuations and the non-zero velocity component normal to the wall.

The dynamics of the response of electrodiffusion probes on fluctuating shear rates has been studied by several authors[5–7]. The analyses coincide in specifying a broad region of conditions – frequencies of flow fluctuations, mean shear rates, and probe sizes – under which the response of the probe reflects just the immediate velocity field of a varying flow. The response of the probe under these (so called quasi-steady) conditions is the same as for a steady flow. Such a transport regime is exclusively assumed in the present study of the normal flow effects. The response of segmented electrodiffusion probes is analyzed for steady three-dimensional velocity fields. A simple two-dimensional flow is considered first to demonstrate the essential features of convective diffusion in the presence of a normal flow com-

ponent. Further, the directional characteristics are computed for segmented circular probes in two-dimensional flows of varying direction which represent an important subclass of the general three-dimensional flows.

Because of problems commonly met in realizing a well-controllable non-viscometric flow, calibrations of real (i.e. geometrically imperfect) segmented probes are limited to the measurements under viscometric conditions. The subject of primary interest in electrodiffusion diagnostics of multiphase flows is to use this calibration information in a way which covers a broader region of flow conditions. It is shown in the discussion how the proposed theory can be used for this aim.

THEORETICAL

Three-Dimensional Kinematics of Flow in the Diffusion Layer

Electrodiffusion probes are used for measurement of local flow characteristics and, therefore, they are constructed as small as possible. This allows to simplify remarkably the relevant mass transfer theory.

The overall transport resistance is concentrated in a thin diffusion layer close to the probe surface. For this reason, the equation of convective diffusion can be considered in the simplified form:

$$(v_x \, \mathrm{d}_x + v_y \, \mathrm{d}_y + v_z \, \mathrm{d}_z) \, c = D \, \mathrm{d}^2_{zz} c \, . \tag{1}$$

The thinness of the diffusion layer allows us to deal with a simplified description of the velocity field close to the wall:

$$\begin{aligned} v_x &= q_x(x, y) \, z \, , \\ v_y &= q_y(x, y) \, z \, , \\ v_z &= -(\mathrm{d}_x q_x + \mathrm{d}_y q_y) \, z^2/2 \, . \end{aligned} \tag{2}$$

The two-dimensional fields q_x, q_y can be linearized over the surface of the probe. The resulting linear representation involves six local kinematic coefficients:

$$\begin{aligned} q_x &= q^0_x + q^0_{xx} x + q^0_{xy} y \, , \\ q_y &= q^0_y + q^0_{yx} x + q^0_{yy} y \, . \end{aligned} \tag{3}$$

We consider here only a three-parameter subclass of linearized spatial velocity fields which fulfil the following conditions:

1) The surface streamlines are parallel each to other at the probe surface, $q^0_y/q^0_x = q^0_{yx}/q^0_{xx} = q^0_{yy}/q^0_{xy}$. This means that we can find a "proper" coordinate system (x', y') for which we have $\mathrm{d}_y q = 0$.

2) There is no vorticity normal to the probe surface, $q^0_{xy} = q^0_{yx}$. This means that q_x depends only on the x coordinate in the "proper" system.

3) There is no critical point at the probe surface, $q_x^2 + q_y^2 > 0$. This means that we have $q_x > 0$ in the "proper" system.

Under these assumptions, the new coordinates (x', y') can be found,

$$x' = x \cos(\Theta) - y \sin(\Theta),$$
$$y' = x \sin(\Theta) + y \cos(\Theta), \tag{4}$$

in which the considered class of linear velocity fields is represented in the following two-dimensional way:

$$v_{x'} = (\bar{q} + 2Ax') z,$$
$$v_{y'} = 0, \tag{5}$$
$$v_z = -Az^2.$$

From the observer's point of view, the kinematics under consideration is represented by the three parameters $\bar{q}$, A, Θ standing for the shear rate magnitude at the probe centre, the normal flow component, and the flow direction relative to the observer's frame of reference, respectively. Note that the origin $(x, y) = (0, 0)$ corresponds always to the probe centre.

Two-Dimensional Case

Let us first assume that the flow direction is known in advance, $\Theta = 0$, and a strip-shaped electrodiffusion probe is placed perpendicular to the flow direction. The corresponding problem of two dimensional convective diffusion was solved in the classical work[8] for arbitrary local shear rates, $q = q(x)$, i.e. for the following two-dimensional velocity field:

$$v_x = q(x) z, \tag{6}$$

$$v_z = -\frac{\mathrm{d}q(x)}{\mathrm{d}x} z^2/2, \tag{7}$$

assuming $q(x) > 0$ for $x \in (x_0, x_L)$, where $x = x_0$ and $x = x_L$ stand for the leading and rear edges of the probe, respectively. For constant bulk concentration c_0 and zero surface concentration of a depolarizer, the resulting expression for limiting diffusion currents is given by[7,8]:

$$i(x_0, x_L) = w \int_{x_0}^{x_L} nFD \, \mathrm{d}_z c\big|_{z=0} \, \mathrm{d}x = kw\left[\int_{x_0}^{x_L} q^{1/2}(x) \, \mathrm{d}x\right]^{2/3}, \tag{8}$$

where w stands for the width of the strip probe in the direction perpendicular to the flow and

$$k = \frac{3^{1/3}}{2\Gamma(4/3)} nFc_0 D^{2/3} . \tag{9}$$

For the viscometric case, $q = \bar{q} = \text{const}$, $A = 0$, this result reduces to the well-known formula given first by Leveque:

$$i^s(x_0, x_L) = i_* \equiv kw\bar{q}^{1/3}L^{2/3} , \tag{10}$$

where L stands for the length of the probe,

$$L = x_L - x_0 . \tag{11}$$

For the linear case, $q = \bar{q} + 2Ax$, we obtain

$$i^s(x_0, x_L) = i_* \left[\frac{(1 + 2x_L\varkappa/L)^{3/2} - (1 + 2x_0\varkappa/L)^{3/2}}{3\varkappa}\right]^{2/3} , \tag{12}$$

where

$$\varkappa = AL/\bar{q} . \tag{13}$$

This result can be further simplified for $\varkappa \to 0$ to provide:

$$i^s(x_0, x_L)/i_* \approx 1 + (\varkappa/3L)[x_0 + x_L] - (\varkappa/3L)^2 [\tfrac{5}{4}(x_0 + x_L)^2 - x_0x_L] - \ldots \tag{14}$$

In particular, if $x = 0$ actually corresponds to the probe centre, $x_0 = -L/2$, $x_L = +L/2$, the asymptote (*14*) reduces to:

$$i^s\left(-\frac{L}{2}, +\frac{L}{2}\right) \approx i_*(1 - \varkappa^2/36 - \ldots) . \tag{15}$$

The total current to a single probe depends nearly exclusively on the mean shear rate $\bar{q}$ and is almost insensitive to the normal flow component.

Let us consider now a probe consisting of two parallel strips, $x \in (-L/2, 0)$ and $x \in (0, +L/2)$, of the same length $L/2$. By using Eq. (*12*), the following two relations

$$(i_1 + i_2)/i_* = \left[\frac{(1 + \varkappa)^{3/2} - (1 - \varkappa)^{3/2}}{3\varkappa}\right]^{2/3} \approx (1 - 0{\cdot}028\varkappa^2) \tag{16a}$$

$$i_2/i_1 = -1 + \left[\frac{(1+\varkappa)^{3/2} - (1-\varkappa)^{3/2}}{1-(1-\varkappa)^{3/2}}\right]^{2/3} \approx 0{\cdot}587(1 + 0{\cdot}450\varkappa + 0{\cdot}094\varkappa^2), \quad (16b)$$

can be derived for the currents, $i_1 = i^s(-L/2, 0)$ and $i_2 = i^s(0, +L/2)$, to the individual strip segments. From these formulae it is obvious that the normal flow parameter A can be determined from the ratio of the partial currents, i.e. the currents to the individual segments. In contrast to the total current $i_1 + i_2$, which is almost independent of A, the ratio i_1/i_2 strongly depends on A and can be used for determination of the normal velocity component. The sensitivity of segmented probes to the normal velocity component is nearly proportional to the size of the probe.

Current to a Sector of a Circular Probe

We shall consider segmented circular probes which consist of several sectors. For the moment we shall consider only a particular orientation of the sectors, as shown in Fig.1. One of the arms of the sector is parallel to the flow direction and its arc forms the leading edge of the probe. As a result, both the shape and orientation are given by two parameters (R, β).

The partial current can simply be calculated by quadratures. The area of the sector is divided into a set of parallel strips of differential width $w = \mathrm{d}y$. Their position relative to a given velocity field is specified by the coordinates $x_0 = x_0(y)$, $x_L = x_L(y)$, see Fig. 1. The angular variable t can conveniently be used instead of the Cartesian one, $y = R \sin(t)$. After the corresponding substitutions in Eq. (*12*), the current $\mathrm{d}i$ to a differential strip is given as

$$\mathrm{d}i = \tfrac{1}{2}k_R f(t) \cos(t)\, \mathrm{d}t\,, \quad (17)$$

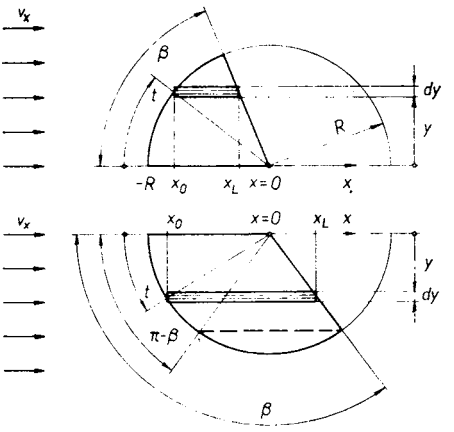

FIG. 1

Geometric parameters of convex sectors of a circle in basic position, i.e. with one of the arms parallel to the flow direction; sector with sharp angle, $0 < \beta < \pi/2$, and sector with obtuse angle, $\pi/2 < \beta < \pi$

where

$$f(t) = \left[\frac{(1 + \varkappa x_L^*)^{3/2} - (1 + \varkappa x_0^*)^{3/2}}{3\varkappa}\right]^{2/3}, \tag{18}$$

$$\varkappa = 2AR/(\bar{q}), \tag{19}$$

$$k_R = k(\bar{q})^{1/3}(2R)^{5/3}, \tag{20}$$

$$x_0^*(t) = x_0(y)/R\,, \quad x_L^*(t) = x_L(y)/R\,. \tag{21}$$

For a sharp-edged sector, $0 < \beta < \pi/2$, we have

$$x_0^* = -\cos(t)\,, \quad x_L^* = -\sin(t)\cot(\beta)\,, \tag{22}$$

and the current can be expressed by a single integral, as follows:

$$\frac{i(\beta)}{k_R/2} = \int_0^{\beta}\left[\frac{\{1 - \varkappa\sin(t)\cot(\beta)\}^{3/2} - \{1 - \varkappa\cos(t)\}^{3/2}}{3\varkappa}\right]^{2/3}\cos(t)\,\mathrm{d}t\,. \tag{23}$$

For a sector with an obtuse angle, $\pi/2 < \beta < \pi$, the function $x_L^*(t)$ consists of two branches for $0 < t < \pi - \beta$ and for $\pi - \beta < t < \pi/2$, see Fig. 1. Consequently, the integration interval must be divided into two parts:

$$\frac{i(\beta)}{k_R/2} = \int_0^{\pi-\beta}\left[\frac{\{1 + \varkappa\sin(t)\cot(\pi - \beta)\}^{3/2} - \{1 - \varkappa\cos(t)\}^{3/2}}{3\varkappa}\right]^{2/3}\cos(t)\,\mathrm{d}t + \\ + \int_{\pi-\beta}^{\pi/2}\left[\frac{\{1 + \varkappa\cos(t)\}^{3/2} - \{1 - \varkappa\cos(t)\}^{3/2}}{3\varkappa}\right]^{2/3}\cos(t)\,\mathrm{d}t\,. \tag{24}$$

The total current to a circular probe can be expressed as the sum of two identical terms $i(\beta)$ for $\beta = \pi$:

$$i_{tot} = 2i(\pi) = k_R\int_0^{\pi/2}\left[\frac{\{1 + \varkappa\cos(t)\}^{3/2} - \{1 - \varkappa\cos(t)\}^{3/2}}{3\varkappa}\right]^{2/3}\cos(t)\,\mathrm{d}t\,. \tag{25}$$

For the special case of no normal flow component, $\varkappa \to 0$, we obtain the known result[5-7]:

$$i_{tot} = i_* \equiv k_R\int_0^{\pi/2}\cos^{5/3}t\,\mathrm{d}t = \frac{(3/2)^{1/3}\,\pi^{1/2}}{\Gamma(11/6)}\,nFc_0D^{2/3}R^{5/3}\bar{q}^{1/3}\,. \tag{26}$$

The effect of the normal flow component on the total current is represented by the

correction factor

$$E(\varkappa) \equiv i_{\mathrm{tot}}(\varkappa)/i_{*} \,. \tag{27}$$

For low and moderate $\varkappa$, E can be expressed by the asymptotic expansion:

$$E(\varkappa) \approx 1 - \frac{2}{99}\varkappa^2 - \frac{1}{309}\varkappa^4 - \ldots \,. \tag{28}$$

This effect is very weak and does not depend on the orientation of the normal flow component (to – or from the surface). The exact values of E are given in Table I.

Let us now consider a convex sector in general, as shown in Fig. 2. The angle $\alpha \in (0, \pi/2)$ and the radius R specify both the shape and size of the sector and the angle Θ indicates its orientation relative to the flow direction. Let us assume the total current i_{tot} to be known for the given velocity field and probe radius R. It is convenient to express the current $i(\Theta, \alpha)$ to the sector in the form

$$i(\Theta, \alpha) = G(\Theta, \alpha)\, i_{\mathrm{tot}} \,, \quad (\varkappa = \mathrm{const}) \,. \tag{29}$$

Let us further define the auxiliar function

$$H(\beta) = i(\beta)/i_{\mathrm{tot}} \,, \quad (\varkappa = \mathrm{const}) \,, \tag{30}$$

for the sector with one of the arms parallel to the flow direction, i.e. for $\alpha = \beta/2$, $\Theta = \beta/2$. The function $H(\beta)$, $0 < \beta < \pi$, can be calculated according to the for-

TABLE I

Effect of the normal flow component on the total current to a circular electrode

$\varkappa$	E	$1 - \frac{2}{99}\varkappa^2$
0	1·0000	1·0000
±0·100	0·9998	0·9998
±0·200	0·9987	0·9987
±0·333	0·9977	0·9978
±0·500	0·9947	0·9949
±0·667	0·9903	0·9910
±1·000	0·9743	0·9798

mulae (*24*)–(*26*). The following three relations specify the basic functional properties of G: its relationship to H

$$G(\beta/2, \beta/2) = H(\beta)\,, \tag{31}$$

the mirror symmetry with respect to the flow direction

$$G(-\Theta, \alpha) = G(+\Theta, \alpha)\,, \tag{32}$$

and the additivity of partial currents

$$G(\Theta, \alpha_1) + G(\Theta + \alpha_1 + \alpha_2, \alpha_2) = G(\Theta + \alpha_2, \alpha_1 + \alpha_2)\,. \tag{33}$$

These relations enable us to express the current to an arbitrary convex sector, $0 < \alpha < \pi/2$, by using only the function H. Assuming $-\pi/2 < \Theta < 2\pi$, we need to consider only the following four cases (Fig. 2):

$$-\alpha < \Theta < \alpha : G(\Theta, \alpha) = H(\Theta + \alpha) + H(\Theta - \alpha)\,, \tag{34a}$$

$$\alpha < \Theta < \pi - \alpha : G(\Theta, \alpha) = H(\Theta + \alpha) - H(\Theta - \alpha)\,, \tag{34b}$$

$$\pi - \alpha < \Theta < \pi + \alpha : G(\Theta, \alpha) = 1 - H(2\pi - \Theta - \alpha) - H(\Theta - \alpha)\,, \tag{34c}$$

$$\pi + \alpha < \Theta < 2\pi - \alpha : G(\Theta, \alpha) = H(2\pi - \Theta + \alpha) - H(2\pi - \Theta - \alpha)\,. \tag{34d}$$

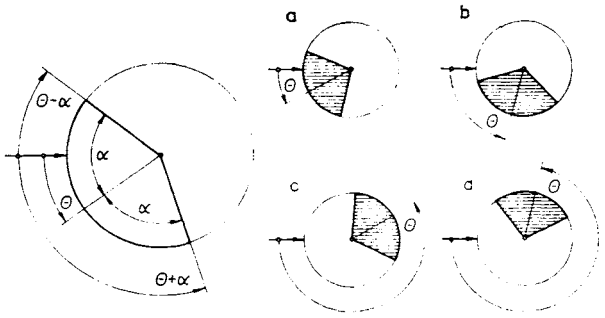

FIG. 2

Geometric parameters of a convex sector of a circle and its four different positions a to d corresponding to Eqs (*34a*) to (*34d*)

RESULTS

Directional Characteristics of the Circular Sectors

Till now, we have considered the current to a sector in a specified position relative to a given two-dimensional velocity field. On the contrary, the directional characteristic specifies the angular dependence of the current to a given sector (α, R = const) under varying flow conditions as represented by the parameters A, $\bar{q}$, Θ:

$$i_s/i_{tot} \equiv F(\Theta, \varkappa) = G(\Theta, \alpha)\,, \quad (\alpha = \text{const};\ \varkappa,\ \Theta \text{ variable})\,. \tag{35}$$

More precisely, the directional characteristics of a segmented probe consist of a set of functions F_s, ($s = 1, 2..$), for the particular sectors of the probe. The sectors need not be of identical shape. Their locations relative to the probe are specified by the angular coordinates Θ_s of their axes.

The directional characteristics of the sectors are commonly represented by their Fourier coefficients:

$$F(\Theta - \Theta_s, \varkappa) = B_0(\alpha_s, \varkappa) + \sum_{m=1}^{\infty} B_m(\alpha_s, \varkappa) \cos\left(m(\Theta - \Theta_s)\right)\,, \tag{36}$$

$$B_0(\alpha_s, \varkappa) = \frac{1}{2\pi} \int_0^{2\pi} F(t, \varkappa)\, \mathrm{d}t\,, \tag{37a}$$

$$B_m(\alpha_s, \varkappa) = \frac{1}{\pi} \int_0^{2\pi} F(t, \varkappa) \cos(mt)\, \mathrm{d}t\,. \tag{37b}$$

The even terms in the Fourier series (*36*) are zero because of the mirror symmetry of the sectors with respect to the axes $\Theta = \Theta_s$. The Fourier series converge very rapidly as manifested by the nearly straigh course of the curves F vs cos (Θ) (Fig. 3).

Empirical Representation of Directional Characteristics

The Fourier coefficients B_m were calculated from the analytical formulae (*23*), (*24*), (*34*), (*37a, b*) for $m = 0 \ldots 10$, $\varkappa \in \langle -1, +1 \rangle$, and $\alpha = \pi/i$, $i = 2 \ldots 9$. The following rules, suggested in our previous work[3],

$$B_0(\alpha, \varkappa) = \alpha/\pi\,, \quad B_m(\alpha, \varkappa) = \sin(m\alpha)\, C_m(\varkappa)\,, \tag{38}$$

were satisfied within the accuracy guaranteed in the numerical computations (roughly to eight decimal digits).

Numerical data on the fundamental Fourier coefficients $C_m(\varkappa)$ are given in Table II. They were further treated by the least squares method to determine the coefficients

of the following polynomial representation:

$$C_m(\varkappa) = C_m(0)\left[1 + \sum_{i=1}^{10} p_{mi}\varkappa^i\right]. \tag{39}$$

Numerical experiments showed that the representation (*39*) with the coefficients given in Table III guarantees the accuracy of F to six valid decimal digits.

Nevertheless, the simple semiempirical formula

$$\begin{aligned} F(\Theta, \varkappa) = \alpha/\pi &+ \left[1 - 0{\cdot}75\varkappa - 0{\cdot}04\varkappa^2\right] 0{\cdot}126 \sin(\alpha)\cos(\Theta) + \\ &+ \left[1 - 1{\cdot}14\varkappa - 0{\cdot}94\varkappa^2\right] 0{\cdot}007 \sin(2\alpha)\cos(2\Theta) - \\ &- \left[1 + 0{\cdot}46\varkappa + 0{\cdot}42\varkappa^2\right] 0{\cdot}003 \sin(3\alpha)\cos(3\Theta) \end{aligned} \tag{40}$$

provides values of F over the full domain of $(\Theta, \alpha, \varkappa)$ accurate to within $\pm 0{\cdot}003$ which

TABLE II

Effect of normal flow component on directional characteristics of radial segments: fundamental Fourier coefficients $C_m(\varkappa)$

$\varkappa$	$100C_1$	$100C_2$	$100C_3$	$100C_4$	$100C_5$	$100C_6$	$100C_7$
1·0	22·081	0·861	−0·228	−0·108	0·058	0·015	−0·013
0·9	20·908	0·927	−0·258	−0·094	0·052	0·017	−0·015
0·8	19·856	0·957	−0·273	−0·086	0·050	0·017	−0·015
0·7	18·870	0·966	−0·281	−0·082	0·050	0·017	−0·015
0·6	17·926	0·960	−0·286	−0·078	0·049	0·017	−0·015
0·5	17·012	0·942	−0·290	−0·075	0·049	0·017	−0·015
0·4	16·118	0·914	−0·292	−0·073	0·049	0·016	−0·015
0·3	15·236	0·875	−0·294	−0·070	0·049	0·016	−0·015
0·2	14·362	0·827	−0·296	−0·068	0·050	0·016	−0·015
0·1	13·490	0·769	−0·299	−0·066	0·050	0·015	−0·015
0·0	12·613	0·701	−0·303	−0·064	0·050	0·015	−0·015
0·1	11·730	0·624	−0·308	−0·062	0·051	0·015	−0·015
0·2	10·833	0·535	−0·316	−0·060	0·051	0·015	−0·015
0·3	9·917	0·434	−0·327	−0·059	0·052	0·014	−0·015
0·4	8·976	0·320	−0·341	−0·059	0·052	0·014	−0·016
0·5	8·003	0·189	−0·361	−0·059	0·053	0·014	−0·016
0·6	6·986	0·038	−0·387	−0·060	0·053	0·014	−0·016
0·7	5·913	−0·136	−0·422	−0·066	0·052	0·013	−0·016
0·8	4·760	−0·342	−0·469	−0·073	0·050	0·013	−0·020
0·9	3·505	−0·595	−0·543	−0·094	0·043	0·010	−0·022
1·0	2·053	−0·929	−0·663	−0·136	0·023	−0·001	−0·024

seems to be acceptable for any practical aims. This conclusion is illustrated in Fig. 3 for the most interesting case of three-segment circular probes, $\alpha = \pi/3$.

DISCUSSION

General Nature of Normal Flow Effects

According to the previous sections, the extent of normal flow effects is characterized by the single dimensionless parameter $\varkappa$. The corresponding normal flow coefficient A in the equation $v_z = -Az^2$ is unambiguously related to longitudinal changes of the shear rate over the electrode surface. The identity

$$A \equiv -\tfrac{1}{2}\,\mathrm{d}^2_{zz} v_z = \tfrac{1}{2}\,\mathrm{d}^2_{zx} v_x = \tfrac{1}{2}\,\mathrm{d}_x q(x) \qquad (41)$$

follows straightforwardly from the continuity equation. In other words, the non-zero normal velocity component close to the probe surface and the longitudinal variation of shaear rates are two unseparable features of the convective process under consideration. The parameter $\varkappa$ can also be expressed in the form

$$\varkappa = \delta q/\bar{q}\,, \qquad (42)$$

where $\delta q = 2AR$ gives the maximum difference between the shear rates at the centre and at the boundaries of the probe. In particular, the cases $\varkappa = \pm 1$ correspond to

TABLE III

Effect of normal flow component on directional characteristics of radial segments: Parameters p_{im} of polynomial expansions to fundamental coefficients, $C_m(\varkappa) = 0{\cdot}01 \sum p_{im}\varkappa^i$

i	p_{im} for m						
	1	2	3	4	5	6	7
1	12·613	0·701	−0·302	−0·063	0·050	0·015	−0·015
2	−8·796	−0·726	−0·045	0·020	0·003	−0·002	−0·000
3	−0·388	−0·493	−0·083	−0·006	0·002	0·005	−0·008
4	−0·701	−0·085	−0·097	−0·021	0·018	−0·006	−0·008
5	−0·165	−0·244	−0·041	−0·040	−0·003	−0·028	0·043
6	−0·777	−0·121	−0·044	0·026	−0·900	0·014	0·036
7	0·121	0·230	0·040	0·063	0·009	0·063	−0·088
8	0·918	0·130	0·076	−0·033	0·142	−0·001	−0·067
9	−0·113	−0·228	−0·061	−0·075	−0·019	−0·047	0·050
10	−0·657	0·092	−0·108	−0·006	−0·090	−0·013	0·034

the extreme conditions where the critical point of flow, $q = 0$, lies on the boundary of the probe.

As shown in the previous section, the simple relation (*26*) between the total current i_{tot} and the mean shear rate $\bar{q}$ holds with an acceptable accuracy even under the aforementioned extreme conditions.

On the contrary, the normal flow component affects the directional characteristics substantially. As shown in Figs 3 and 4, the ratios of the maxima to the minima on the directional characteristics change strongly with $\varkappa$. Because just the ratios are essential for determining the flow direction, it can be said that the normal flow component affects the directional sensitivity of segmented probes. In particular, the sensitivity falls down considerably in the proximity of forward critical points, $\varkappa \to 1$. Close to rear critical points, $\varkappa \to -1$, the directional sensitivity is even larger than in the viscometric case, $\varkappa$.

Normal flow Effects in Determining the Flow Direction

The segmented probes are used primarily in determining the flow direction. We discuss here exclusively the three-segment probes, as three segments represent the minimum number sufficient to determine the flow direction unambiguously.

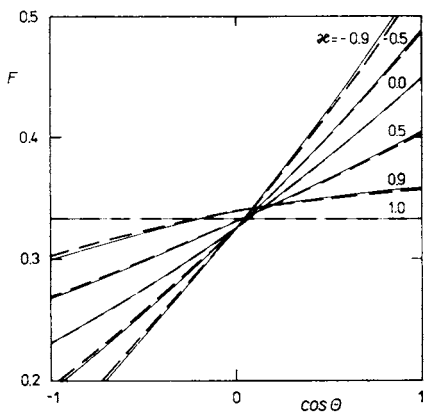

FIG. 3

Directional characteristics for a sector of a geometrically perfect three-segment circular probe, $\alpha = \pi/3$; solid lines — exact courses; dashed lines — empirical approximation, Eq. (*40*)

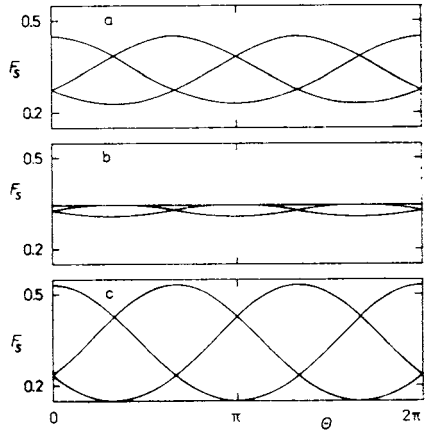

FIG. 4

Complete directional characteristic of geometrically perfect three-segment probe under: a the viscometric condition, $\varkappa = 0$; b conditions close to the forward hydrodynamic critical point, $\varkappa = 0{\cdot}9$; c conditions close to the rear hydrodynamic critical point, $\varkappa = -0{\cdot}9$

From the mathematical standpoint the problem consists in solving the non-linear system of four equations

$$i_1/(i_1 + i_2 + i_3) = F_1(\Theta, \varkappa)\,, \tag{43a}$$

$$i_2/(i_1 + i_2 + i_3) = F_2(\Theta, \varkappa)\,, \tag{43b}$$

$$i_3/(i_1 + i_2 + i_3) = F_3(\Theta, \varkappa)\,, \tag{43c}$$

$$i_1 + i_2 + i_3 = i_*(\bar{q})\, E(\varkappa)\,, \tag{43d}$$

with the terms on the left-hand side known from measurements. Note the obvious constraint $F_1 + F_2 + F_3 = 1$. The subscripts 1, 2, 3 refer to the three individual segments. The functions E, i_*, F_s, $s \in [1, 2, 3]$ must be known. For the moment, the probes are assumed to consist of geometrically ideal segments (sectors); the functions on the right-hand side of Eqs (*43*) are hence given by the theory. Three degrees of freedom in the equations correspond to the three unknown parameters Θ, $\varkappa$, $\bar{q}$.

The questions of existence, uniqueness, and parametric sensitivity of the solution are of primary importance, as the experimentally obtained terms on the left-hand side can be strongly affected by experimental errors. Instead of a thorough analysis of the problems suggested, we shall show an algorithm which guarantees the solvability of the system (*43a–d*) for any admissible set of input data and implies an admissibility check as well.

In the first step, the subscripts are ordered according to the magnitudes of the corresponding partial currents,

$$i_p < i_q < i_r\,. \tag{44}$$

It is obvious from the typical examples of complete directional characteristics given in Fig. 4 that the ordered triple of the segment subscripts $[p, q, r]$ specifies the flow direction Θ within an ambiguity less than 60°. In other words, six permutations of the subscripts 1, 2, 3 are in one-to-one relation to the six angle subintervals which fully cover the 360°-range of all possible flow directions.

This feature has been used in our previous work[3] for constructing an efficient algorithm for treating the data taken under viscometric conditions. The same algorithm will work even under the considered three-parametric class of flow conditions because the changes of $\varkappa$ affect primarily the span between maximum and minimum partial currents, leaving the general structure of the complete directional characteristics essentially unchanged. This invariance is obvious from Fig. 3 for the three-segment probes. As a result, the first guess locates Θ into one of the six fixed subintervals.

This guess is further improved in the second step. The ratio i_r/i_p can vary from unity (for the extreme case $\varkappa = 1$) to the theoretical maximum $G(\Theta)/G(\Theta \pm 2\pi/3) \approx$

≈ 3 (for the other extreme case $\varkappa = -1$). If this ratio is beyond the given limits, the corresponding experimental point has been determined incorrectly and must be cancelled. Any of the ratios i_a/i_b, $(a, b) \in [1, 2, 3]$, is independent of the shear rate magnitude $\bar{q}$ and depends only on $(\Theta, \varkappa)$, as explicitely marked in Eqs (*43a–c*). For solving the problem, it is sufficient to consider only two independent linear combinations of these equations, as the third one is redundant because of the constraint $\sum_s F_s = 1$. The choice of these combinations can strongly affect the efficiency of the resulting algorithms. The algorithm actually suggested is based on the fact that the following two combinations

$$K \equiv [i_r - i_p])/[i_p + i_q + i_r], \tag{45a}$$

$$T \equiv [i_q - (i_p + i_r)/2]/[i_r - i_p], \tag{45b}$$

depend nearly selectively on only one of the unknown parameters, Θ and $\varkappa$. This is documented in Figs 5 and 6, where the plots of the corresponding theoretical functions

$$K^*(\varkappa, \Theta) \equiv F_r(\Theta, \varkappa) - F_p(\Theta, \varkappa) = 2F_r(\Theta, \varkappa) + F_q(\Theta, \varkappa) - 1, \tag{46a}$$

$$T^*(\Theta, \varkappa) \equiv \frac{2F_q(\Theta, \varkappa) - F_p(\Theta, \varkappa) - F_r(\Theta, \varkappa)}{2[F_r(\Theta, \varkappa) - F_p(\Theta, \varkappa)]} = \frac{\frac{3}{2}F_q(\Theta, \varkappa) - \frac{1}{2}}{2[F_r(\Theta, \varkappa) + F_q(\Theta, \varkappa)] - 1} \tag{46b}$$

are given.

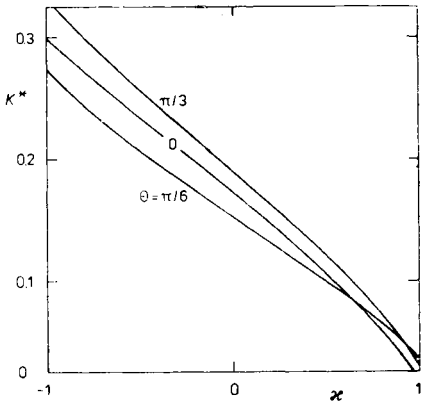

FIG. 5

Combinations K^* of the currents to individual segments at different values of Θ

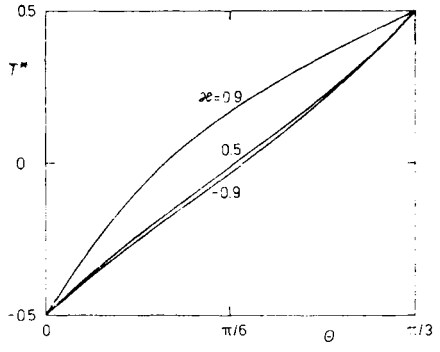

FIG. 6

Combinations T^* of the currents to individual segments at different values of $\varkappa$

As K depends only slightly on Θ, the single equation

$$K = K^*(\varkappa, \Theta) \tag{47a}$$

provides a good estimate of $\varkappa$ even for a rough estimate of Θ. An analogous conclusion can be drawn concerning the equation

$$T = T^*(\Theta, \varkappa) \tag{47b}$$

which provides a good estimate of Θ for a rough estimate of $\varkappa$.

As a result, an efficient algorithm for the second step is based on the iteration loop which consists of solving alternately the equations $K = K^*(\varkappa, \Theta)$ and $T = T^*(\Theta, \varkappa)$ with known values of K, T. The solving routines can be constructed to work fast enough, as the functions $K^*(\varkappa, \Theta)$ and $T^*(\Theta, \varkappa)$ are monotonous and nearly linear with respect to their first arguments (Figs 5 and 6). The remaining parameter $\bar{q}$ can be expressed explicitly from Eq. (*43d*).

Calibration Data via Extrapolating the Viscometric Information

Real segmented electrodiffusion probes are far from being geometrically perfect. Individual segments differ in their shapes and areas. There are insulating insertions of finite thickness between them. Consequently, a calibration procedure must be used to determine the functions $i_*(\bar{q})$, $E(\varkappa)$, $F_s(\Theta, \varkappa)$.

Until now, reliable procedures for the experimental calibration of electrodiffusion probes have been developed only for measurements under viscometric conditions[1-4], i.e. for $\varkappa = 0$. We suggest here a semiempirical procedure for obtaining the functions $i_s(\bar{q})$, $E(\varkappa)$, $F_s(\Theta, \varkappa)$ by an extrapolation of the viscometric calibration data.

Let us first assume that a three-segment probe consists of geometrically perfect circular sectors with different angles α_s. Then, the representation of the directional characteristics can be written in the following form:

$$F_s(\Theta, \varkappa) = \alpha_s/\pi + \sum_m B_m(\alpha_s, \varkappa) \cos\left[m(\Theta - \Theta_s)\right], \tag{48}$$

where the individual sectors, $s \in [1, 2, 3]$, are distinguished by their angles α_s and angular shifts Θ_s relative to the reference frame, $\Theta = 0$, of the entire probe. It follows from the rules (*38*) that $B_m(\alpha_s, \varkappa)$ can be expressed in the form

$$B_m(\alpha_s, \varkappa) = h_m(\varkappa)\, B_m(\alpha, 0), \tag{49}$$

where the coefficients $h_m(\varkappa) = C_m(\varkappa)/C_m(0)$ are independent of α.

The formula (*48*) can also be written in the following way:

$$F_s(\Theta, \varkappa) = f_{s0} + \sum_m h_m(\varkappa) \left[f_{sm} \cos(m\Theta) + g_{sm} \sin(m\Theta) \right], \qquad (50)$$

where the coefficients f_{sm}, g_{sm} depend exclusively on the angular sizes α_s of the individual segments and their angular shifts Θ_s. These coefficients can be determined either from the theory or by a calibration experiment under viscometric conditions. In any case, the coefficients h_m are calculated according to the theory, see Table III and Eq. (*40*). For the probes consisting of circular sectors of different angles, the suggested procedure provides correct calibration data, assuming negligible effect of insulating gaps between the segments. We expect that this procedure will provide acceptable results for real electrodiffusion as well, because any effects of microscopic imperfections of the active segments and the insulating gaps are involved in the starting calibration data obtained experimentally under viscometric condition.

CONCLUSIONS

The total limiting diffusion current to a segmented electrode depends nearly exclusively on the shear rate $\bar{q}$ at the centre of the probe. The normal velocity component and the corresponding changes of the local wall shear rate have only minor effect.

The ratios of the currents to individual segments of a three-segment electrodiffusion probe are extremely sensitive to both the flow direction and the normal flow component. By using the algorithm suggested in the present work, the triple signal can be processed to obtain data about these two additional kinematic parameters. A semiempirical method is suggested for the application of this algorithm to real probes by using only the viscometric calibration data.

The authors are indebted to Dr Pavel Mitschka for his helpful criticism during the preparatory stage of this article.

LIST OF SYMBOLS

A	normal flow coefficient, Eq. (*5*)
$B_m(\alpha, \Theta)$	Fourier coefficients of directional characteristic, Eqs (*37*), (*38*)
$C_m(\varkappa)$	fundamental Fourier coefficients, Eqs (*38*), (*39*), Table II
$c(x, y, z)$	concentration field of depolarizer
c_0	bulk concentration of depolarizer
D	diffusivity of depolarizer
d_x, d_y, d_z	partial derivatives
$E(\varkappa)$	correction of total currents for normal flow effects, Eqs (*27*), (*28*), Table I
$F(\Theta, \varkappa)$	directional characteristic of a given circular sector, Eqs (*35*), (*36*)
$F_s(\Theta, \varkappa)$	directional characteristic of s-th segment of circular probe, Eq. (*48*)
f_{sm}, g_{sm}	m-th Fourier coefficients for s-th segment under viscometric condition, Eq. (*50*)
$G(\Theta, \alpha)$	normalized current to a circular sector under given flow condition, Eqs (*29*), (*34*)

$h_m(\varkappa)$	correction of m-th Fourier coefficients for normal flow effects, Eq. (*49*)
$H(\beta)$	normalized current to circular sectors in basic position, Eqs (*30*), (*31*), (*34*)
$i(\beta)$	current to circular sectors in basic position, i.e. with one of its arms parallel to the flow direction
$i(\Theta, \varkappa)$	current to a segment, Eq. (*29*)
$i^s(x_0, x_L)$	current to a strip
i_{tot}	total current to a probe
i_*	total current under viscometric condition to a strip probe, Eq. (*10*), or a circular probe, Eq. (*26*)
i_k	partial currents to strip segments
i_s	partial currents to segments of a circular probe
k	transport coefficient for a strip, Eqs (*8*), (*9*)
k_R	transport coefficient for a circle, Eqs (*17*), (*20*)
K	Θ-insensitive combination of partial currents, Eq. (*45a*)
K^*	theoretical representation of K, Eq. (*46a*)
L	length of a strip probe along the flow
nF	electric charge corresponding to the electrochemical conversion of 1 mole of a depolarizer
p_{im}	coefficients in the polynomial representation of $C_m(\varkappa)$, Eq. (*39*), Table III
$q(x)$	longitudinal profile of shear rates
$\bar{q}$	shear rate magnitude at the probe centre
R	radius of a circular probe
t	angular variable
T	$\varkappa$-insensitive combination of partial currents, Eq. (*45b*)
T^*	theoretical representation of T, Eq. (*46b*)
v_x, v_y, v_z	velocity components
x	longitudinal coordinate (parallel the flow)
x_0, x_L	x coordinates of the leading and rear edges of a strip, Fig. 1
y	transversal coordinate (across the flow)
z	normal coordinate (perpendicular to the wall)
w	strip width (across the flow)
α	angular size of a circular sector, Fig. 2
β	angle of a circular sector in basic position, Fig. 1
Θ	angular shift of a segment or of a probe, Fig. 2
Θ_s	angular shifts of the segments constituting circular probe, Eq. (*48*)
$\varkappa$	dimensionless measure of the normal flow effects, Eqs (*13*), (*19*)

REFERENCES

1. Menzel Th., Sobolík V., Onken U., Čermák J.: *Electrodiffusion Probe for Direction-Specific Shear Rate Measurement. 8th Int. Congress CHISA, Prague 1987.*
2. Bergerhoff J.: *Thesis.* Universität Dortmund, Dortmund 1987.
3. Wein O., Sobolík V.: Collect. Czech. Chem. Commun. *52*, 2169 (1987).
4. Menzel Th., Sobolík V., Wein O., Onken U.: Chem.-Ing.-Tech. *59*, 492 (1987).
5. Hanratty T. J., Campbell J. A. in: *Fluid Mechanics Measurements* (R. J. Goldstein, Ed.). Hemisphere, Washington 1983.
6. Nakoryakov V. E., Burdukov A. P., Kashinsky O. N., Geshev P. I.: *Electrodiffusion Method of Investigation of Turbulent Flows.* Institute of Thermophysics, Novosibirsk 1986.

7. Pokryvaylo N. A., Wein O., Kovalevskaya N. D.: *Electrodiffusion Diagnostics of Flow in Suspensions and Polymer Solutions.* Nauka i Tekhnika, Minsk 1988.
8. Lighthill M. J.: Proc. R. Soc. London, A *202*, 359 (1950).

Translated by the author (O.W.).